Recent Developments in Characterization of Ion-Exchange Membrane Processes: Impedance Spectroscopy for a Concentration Polarized Boundary Layer

Jin-Soo Park, Seung-Hyeon Moon*
Department of Environmental Science and Engineering
Kwangju Institute of Science and Technology (K-JIST)
[1]Department of Chemical Engineering, Kongju National University

Introduction. Ion-exchange membranes have been widely used in various applications such as diffusion dialysis, electrolysis, electrodialysis, fuel cell, etc [1-2]. When an electric current passes through the membrane system, the current is carried by both positive and negative ions in the bulk solution phases, whereas it is carried mainly by the counter-ions in the membrane. Moreover, the difference in transport number of the counter-ions between the bulk solution phases and the membrane leads to depletion in the electrolyte concentration on the dilute side and to enrichment on the concentrate side. As a result, concentration polarization arises from the interface between the ion-exchange membrane and the electrolyte solutions, and the polarized layers such as a diffusion boundary layer (DBL) are formed on the membrane surface. Impedance spectroscopy is often used to characterize a wide variety of electrochemical phenomena concerning solid state, porous materials, synthetic and biological membranes, and liquid electrolytes [5]. Moreover, it provides valuable information on the functional and structural characteristics of membrane systems. In this study, we examined impedance spectra of a concentration-polarized ion exchange membrane system (CPIEMS) in light of its main dielectric and phenomenological structures. I-V curves were measured for ion-exchange membrane systems in the absence and presence of BSA on KCl. Based on the results, various electrochemical parameters were determined to characterize the fouling phenomena by BSA. Using alternating current offset by direct current, impedance

spectra were obtained to identify the structural change of the BSA fouling layer deposited on the surface of the AEM

Materials and methods. Neosepta CMX and AMX (Tokuyama Soda Co., Japan) are reinforced standard grade homogenous ion-exchange membranes. Lyophilized bovine serum albumin (BSA) powder (98% purity; Sigma, St. Louise, Missouri) and potassium chloride (Sigma, St. Louise, Missouri) in reagents grade was used as a foulant and a supporting electrolyte, respectively. Deionized water (18 MΩ-cm) was used in preparing all the electrolytes. Impedance spectroscopy was carried out on these membranes using a two-compartment electrodialytic cell with compartments of equal volume (150 mL) with the membrane supported in a circular hole between the compartments. The effective area of the membrane was 0.785 cm^2. The impedance of the membrane system was measured using two Ag/AgCl voltage electrodes immersed into Luggin capillaries and separate Ag/AgCl electrodes for injecting the current. I-V curves for the AMX and CMX in the 0.01 M KCl solution in the presence of 1 wt% BSA were determined using a six-compartment electrodialysis cell made of Plexiglas. The effective membrane area of the electrodialysis cell was 25 cm^2. The streams of **3-1** and **3-2** (see Fig. 1) with 500 mL of the 0.05 M KCl solution in the presence of 1 wt% BSA (i.e., feed solutions) were circulated in the same reservoir at a flow rate of 50 mL/min.

Results and Discussion. Fig. 2 shows the typical Nyquist plot of the CPIEMS used in this study. At lower frequencies (below 139 Hz), the diameter of the second capacitive loop decreased in the presence of stirring, corresponding to the impedance by ion diffusion in the DBL. This implies that the first capacitive and the following inductive loop were due to the geometric effect of the electrochemical cell. Those loops were also affected by concentration of the electrolyte and distance between the two reference Ag/AgCl electrodes. It is considered that their electrical responses to the dielectric and phenomenological structures of the CPIEMS can be described as the basic electrical

circuit components such as resistors and capacitors in series or parallel. The shift of the beginning part of the second capacitive loop toward lower real impedance and the decrease in their size are due to an increase in solution conductance. It is inferred that there is another impedance to restrict ionic transport from the solution phase to the membrane phase (i.e., heterogeneous transport of the counter-ions [6]). The size of the inductive loop increases with decreasing the distance between the two reference electrodes, because of the effect of the mutual inductance diminishes at a long distance. On the other hands, the capacitive loop decreases with increasing the inductive one. The increased resistance with increasing the distance causes the shift of the second capacitive loop as similar as the effect of the concentration, but the size of the circle including two capacitive loops and an inductive one do not seem to change, only the fraction of the capacitive loop and the following inductive one changed. This implies that the loops by the geometric effect are mainly caused by the solution resistance and the mutual inductance.

The current-voltage curves for the AMX and CMX in the two different solutions are shown in Fig. 3. Choi et al. reported that the surface of ion-exchange membrane consisted of conducting and non-conducting region though it was homogeneously manufactured [7]. It was expected that the heterogeneity of an anion-exchange membrane particularly increased in the presence of BSA since the negatively charged BSA was electrostatically favor to be interacted with the positively charged functional group of anion-exchange membrane. As a result of chronopotentiometry, the heterogeneity of both the ion-exchange membranes increases as shown in Table 1. In case of the AMX membrane in the 0.01 M KCl and 1wt.% BSA solution, however, the severer heterogeneity was attained. As expected, BSA adsorption occurs chemically on the surface of the CMX membrane and both chemically and electrostatically on the surface of the AMX membrane. Therefore, the further calculations for the electrochemical properties of the ion-exchange membranes obtained from the current-voltage curves should consider the fraction of conducting region of the ion-exchange membranes. The thickness of effective DBL

shows a clear-cut of the BSA fouling on the AMX membrane only as shown in Table 1. There is no difference for the thickness of effective DBL in case of the CMX membrane, but about 110 μm increase is shown by the BSA fouling in the case of the AMX membrane.

Fig. 4 shows the impedance spectra for the AMX membrane in the two test solutions at four different current densities superimposed on the AC perturbation, based upon the corresponding limiting current densities (LCD). Fig. 4a and 4b show the similar impedance spectra trend (the second capacitive loop), and just the impedance intensity is increased due to the formation of severe concentration polarization by a current density increase until LCD. However, in the over LCD regions, an additional capacitive loop and Warburg impedance are added in Fig. 4c and additional capacitive and inductive loop in Fig. 4d following the second capacitive loop. As shown in Fig. 3, it is noted that the two distinguishable slopes appear in the over LCD region for the AMX membrane in the 0.01 M KCl and 1 wt.% BSA solution. The over LCD region was divided into two groups, and the impedance spectra of each group was investigated (see Fig. 4c and 4d, respectively). The notable difference between the two impedance data might be caused by a structural change of the deposited BSA on the surface of the AMX membrane. It could be expected that the BSA adsorbed on the surface of the AMX membrane became denser at higher electrical power and formed a compressible deposit in the first over LCD region. The AMX membrane with the compressible BSA deposit became the bipolar structure, and water dissociation might be enhanced. Finally, the negatively charged compressible BSA deposit reacted with the proton dissociated at the bipolar structure, and became neutral. This might decrease resistance of the second over LCD region and cause the different impedance spectra as shown in Fig. 3 and Fig. 4, respectively. The pH of the solution in the presence of BSA shows the more stable variation than that in the absence of BSA due to the buffering effect. In this regard, it was expected that the pH change underestimated the amount of protons and hydroxide ions generated between the deposited BSA and the AMX membrane. Nevertheless, the greater change in pH with time is shown at the over LCDs due to enhancement of

water-splitting phenomena. Moreover, the greater amount of the generated protons might completely neutralize the negatively charged BSA deposit, causing to lower the resistance in the second LCD region of the I-V curve (see Fig. 3). Hence, we suggest that the electrochemically connected the equivalent circuits in the absence and presence BSA on KCl solution were formed the three and four components respectively as shown the Fig. 5.

Conclusions. BSA fouling phenomena in the AEM system were mainly investigated using I-V curves by direct current and impedance spectroscopy by offset alternating current. From the I-V curve results, it was found that the fraction of the conducting region was significantly affected by the BSA fouling, and played an important role in determining the electrochemical parameters of ion-exchange membranes. The impedance spectroscopic study explained that the current density highly influenced the structure of BSA-fouling layer deposited on the surface of AEM. It resulted in the formation of the bipolar structure to enhance the water splitting phenomena. Because of the enhancement of the water splitting phenomena between the BSA-fouling and the AEM, the negatively charged BSA-fouling layer became neutral by the protons. It is indicated that the decrease in resistance in the I-V curve and the inductive loop on the impedance spectra. The main fouling phenomenon in the separation processes using ion-exchange membranes is the formation of fouling layers on the surface. It is concluded that the I-V relation by direct current and impedance spectroscopic study by the offset alternating current can be a useful approach to investigate ongoing fouling phenomena, and enables to provide important information on operations of electrodialysis processes to minimize fouling effects.

Acknowledgement. This work was supported by the National Research Laboratory (NRL) Program of Korea Institute of Science and Technology Evaluation and Planning (KISTEP) (Project No. 2000-N-NL-01-C-185).

References.

1. E.-G. Lee, S.-H. Moon, Y.-K. Chang, I.-K. Yoo and H.-N. Chang, J. Membr. Sci., 145 (1998) 53.
2. M.-S. Kang, K.-S. Yoo, S.-J. Oh, and S.-H. Moon, J. Membr. Sci., 188 (2001) 61
3. J.-S. Park, H.-J. Lee, S.-J. Choi, K.E. Geckeler, J. Cho, and S.-H. Moon, J. Colloid Interf. Sci., 259 (2003) 293.
4. J.-S. Park, H.-J. Lee, S.-H. Moon, Sep. Purif. Tech., 130 (2003) 102.
5. H.-J. Lee, J.-H. Choi, J. Cho and S.-H. Moon, J. Membr. Sci., 203 (2002) 115.
6. R.F.D. Costa, J.Z.F. Ferreira and C. Deslouis, J. Membr. Sci., 215 (2003) 115.
7. J.H. Choi, S.H. Kim, and S.H. Moon, J. Colloid Interf. Sci., 241(1), 120 (2001).

Table 1. Effective physicochemical parameters on the two ion-exchange membranes (CMX, AMX) in the two different types of solution by the consideration of fraction of conducting phase of ion-exchange membranes.

Membrane	Solution	Fraction of conducting phase (ε)	Effective I_{lim}^{*} ($=I_{lim}/\varepsilon$) [A/m^2]	Thickness of DBL [μm]	Thickness of effective DBL [μm]
CMX	0.01 M KCl	0.98	10.63	385.5	377.9
	0.01 M KCl + 1% BSA	0.84	15.83	443.6	372.7
AMX	0.01 M KCl	1.0	12.48	334.2	334.2
	0.01 M KCl + 1% BSA	0.019	437	22432	448.6

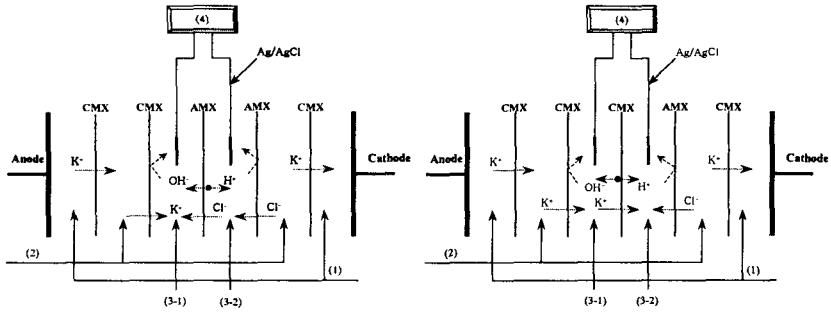

(a) (b)

Figure 1. Schematic diagrams of the six-compartment cell for I-V curve measurement and water splitting experiments of (a) the CMX membrane and (b) the AMX membrane: (1) electrode solution (0.5 M K_2SO_4), (2) 0.5 M KCl, (3) feed solution, (4) multimeter (the central membrane is the test membrane)

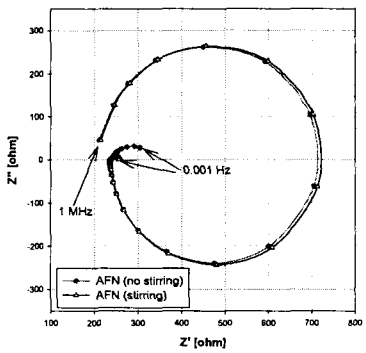

Figure 2. Effect of cell geometric capacitance on impedance spectroscopy (10 mA amplitude, frequency range from 10^6 to 10^{-3}).

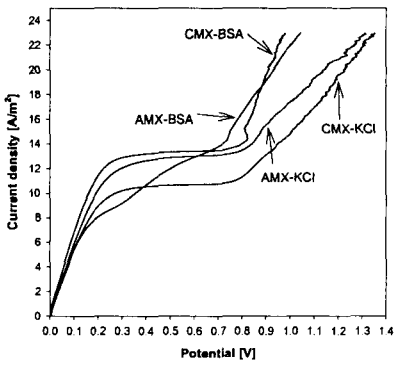

Figure 3. I-V curves of 0.01 M KCl with the existence of 1% BSA for the Neosepta CMX and AMX and their fittings by Equation when dc power is applied.

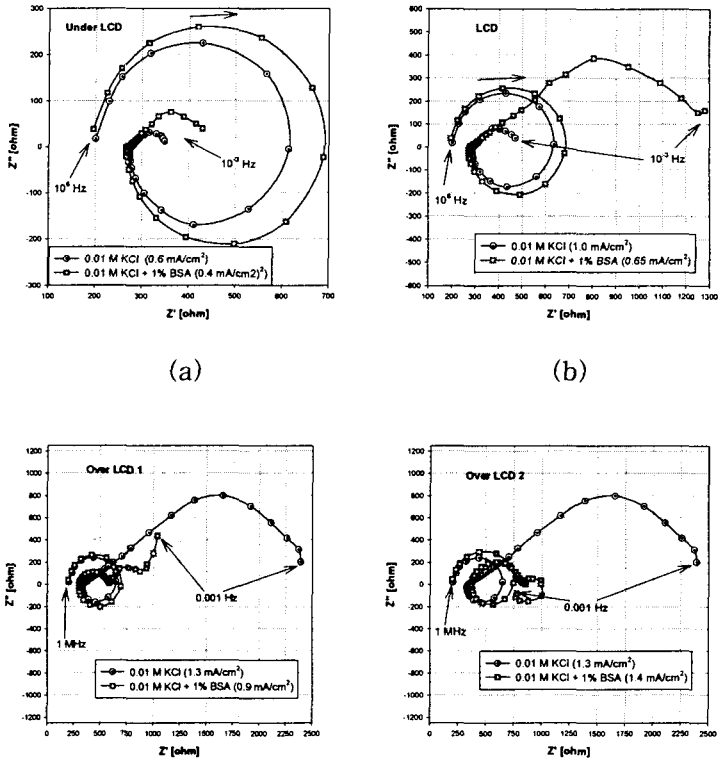

Figure 4. Comparison of the impedance spectroscopy of the 0.01 M KCl solution and the 0.01 M KCl/1 wt.% BSA solution (10 mA amplitude, frequency range from 10^{6} to 10^{-3}): (a) under LCD (b) LCD (c) first over LCD (d) second over LCD.

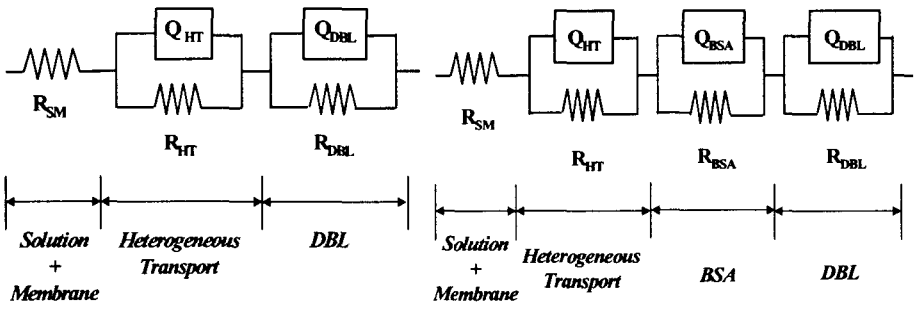

Figure 5. Equivalent circuits for the ion-exchange membrane systems in the (a) absence and (b) presence of BSA, consisting of effects of the membrane immersed in solution (SM), heterogeneous ionic transport (HT), BSA-fouling (BSA) and diffusion boundary layer (DBL).